

This article is published as part of the *Dalton Transactions* themed issue entitled:

New Horizons in Organo-f-element Chemistry

Guest Editor: Geoff Cloke
University of Sussex, UK

Published in [issue 29, 2010](#) of *Dalton Transactions*

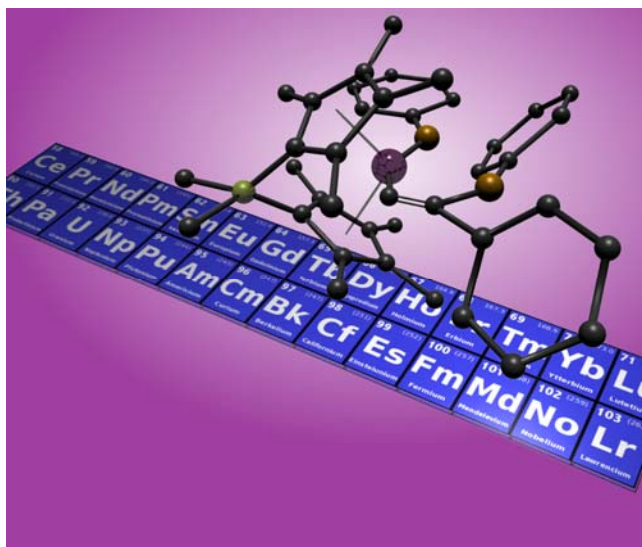


Image reproduced with the permission of Tobin Marks

Articles in the issue include:

PERSPECTIVES:

[Organo-f-element catalysts for efficient and highly selective hydroalkoxylation and hydrothiolation](#)

Charles J. Weiss and Tobin J. Marks, *Dalton Trans.*, 2010, DOI: 10.1039/c003089a

[Non-classical divalent lanthanide complexes](#)

François Nief, *Dalton Trans.*, 2010, DOI: 10.1039/c001280g

COMMUNICATIONS:

[A bimetallic uranium \$\mu\$ -dicarbide complex: synthesis, X-ray crystal structure, and bonding](#)

Alexander R. Fox, Sidney E. Creutz and Christopher C. Cummins
Dalton Trans., 2010, DOI: 10.1039/c0dt00419g

PAPERS:

[Coordination polymerization of renewable butyrolactone-based vinyl monomers by lanthanide and early metal catalysts](#)

Garret M. Miyake, Stacie E. Newton, Wesley R. Mariott and Eugene Y.-X. Chen,
Dalton Trans., 2010, DOI: 10.1039/c001909g

Visit the *Dalton Transactions* website for more cutting-edge inorganic and organometallic chemistry research

www.rsc.org/dalton

Rare-earth metal bis(tetramethylaluminate) complexes supported by a sterically crowded triazenido ligand†

Rannveig Litlabø,^a Hyui Sul Lee,^b Mark Niemeyer,^b Karl W. Törnroos^a and Reiner Anwander^{*a,c}

Received 8th December 2009, Accepted 23rd January 2010

First published as an Advance Article on the web 12th March 2010

DOI: 10.1039/b925837j

Complexes $[\text{NNN}]\text{Ln}(\text{AlMe}_4)_2$ (Ln = Y, La, Nd, Lu) bearing the sterically demanding aryl-substituted triazenido ligand $[(\text{Tph})_2\text{N}_3]$ (Tph = [2-(2,4,6-*i*-Pr₃C₆H₂)C₆H₄]) can be obtained from homoleptic complexes $\text{Ln}(\text{AlMe}_4)_3$ in moderate yields, both *via* protonolysis with $[(\text{Tph})_2\text{N}_3]\text{H}$ and a salt metathesis reaction pathway utilizing $[(\text{Tph})_2\text{N}_3]\text{K}$. In the solid state the Y and Lu derivatives are isostructural, with both tetramethylaluminate groups coordinated in an η^2 fashion, while one of the $[\text{AlMe}_4]$ ligands of the Nd derivative features a distorted η^2 coordination mode. Due to the high affinity of the triazenido ligand toward the more Lewis-acidic and harder aluminium cation compared to the softer rare-earth metal centres, ligand redistribution is observed in solution and formation of byproduct $[(\text{Tph})_2\text{N}_3]\text{AlMe}_2$ is prominent. While the monoanionic triazenido ligand coordinates the rare-earth metal centres in an asymmetrical *syn/anti* fashion, it adopts an almost symmetric *syn/syn* configuration in the aluminium complex. Attempts were also made to produce putative dimethyl complexes $\{[(\text{Tph})_2\text{N}_3]\text{LnMe}_2\}$ (Ln = Y, Lu) *via* cleavage of the aluminate moieties with diethyl ether. Furthermore, the intrinsic redistribution reactions are proposed to affect the performance of complexes $[(\text{Tph})_2\text{N}_3]\text{Ln}(\text{AlMe}_4)_2$ in isoprene polymerization.

Introduction

N-coordinating (chelating) ligands provide unique scaffolds for the synthesis and isolation of highly reactive monomeric organometallic reagents.¹ Importantly, d-transition and rare-earth metal complexes supported by such ancillary ligands emerged as highly efficient catalysts for the enantioselective fabrication of polymers and fine chemicals.² More specifically, rare-earth metal bis(alkyl) complexes containing amidinato,³ β -diketiminato,⁴ aminopyridinato,⁵ aza-crown,⁶ and other *N*-coordinating ancillary ligands⁷ have proved themselves active in the polymerization of 1,3-dienes, ethylene, and α -olefins upon activation by organoboron and/or organoaluminium cocatalysts.

Although monoanionic triazenido ligands are structurally related to amidinato ligands, their utilization in organometallic catalysis is scarce.⁸ Since triazenido ligands are weaker donors than the isoelectronic amidinato and the related β -diketiminato ligands, enhanced electrophilicity of the metal centres can be anticipated, and hence different reactivity.⁹ In rare-earth metal chemistry, X-ray structurally authenticated examples are limited to the solvated phenyl-substituted triazenide complexes $\text{Ln}^{\text{III}}[(\text{C}_6\text{H}_5)_2\text{N}_3]_3(\text{NC}_5\text{H}_5)_2$ and $\text{Cp}_2\text{Ln}^{\text{III}}[(\text{C}_6\text{H}_5)_2\text{N}_3](4\text{-}t\text{BuNC}_5\text{H}_4)$ (Ln = Er, Lu),¹⁰ and the unsolvated pentafluorophenyl derivatives $[(\text{Dmp})(\text{Tph})\text{N}_3]\text{Ln}^{\text{III}}(\text{C}_6\text{F}_5)$ (Dmp = [2,6-(2,4,6-

$\text{Me}_3\text{C}_6\text{H}_2)_2\text{C}_6\text{H}_3]$; Tph = [2-(2,4,6-*i*-Pr₃C₆H₂)C₆H₄]; Ln = Eu, Yb).¹¹ In addition asymmetric mesityl azido and adamantyl azido ligands afforded complexes $[\text{L}(\text{MesN}_3)]\text{Ln}[(\text{MesN}_3)(\text{CH}_2\text{SiMe}_3)_2]$ (Ln = Lu, Sc; L = (2,6-Me₂C₆H₃)NCH₂C₆H₄P(C₆H₅)₂)¹² and $(\text{C}_5\text{Me}_5)_2\text{La}[\eta^2\text{-}(N,N')\text{-}(\text{C}_5\text{Me}_5)\text{NN}'\text{N}''\text{Ad}](\text{N}_3\text{Ad})$,¹³ respectively.

We have recently shown that homoleptic complexes $\text{Ln}(\text{AlMe}_4)_3$ (Ln = Y, La, Nd, Lu) can be used as precursors for the synthesis of non-cyclopentadienyl complexes with donor-functionalized diamido $[\text{NON}]^{2-}$ and $[\text{NNN}]^{2-}$, imino-amido $[\text{NNN}]^-$, as well as tris(pyrazolyl)borato (Tp) $[\text{NNN}]^-$ ancillary ligands.^{5b,14} Herein we add to this tetramethylaluminate-based postmetallocene library¹⁵ the triazenido ligand $[(\text{Tph})_2\text{N}_3]$,¹⁶ and show how rare-earth metal bis(tetramethylaluminate)s can be obtained by two complementary reaction protocols, namely alkane elimination and salt metathesis.^{14b,17} We also report on our attempts to synthesize dimethyl complexes of the type $[(\text{Tph})_2\text{N}_3]\text{LnMe}_2$ *via* donor-induced cleavage of the tetramethylaluminate moieties in $[(\text{Tph})_2\text{N}_3]\text{Ln}(\text{AlMe}_4)_2$. And finally, we describe how the latter rare-earth metal bis(tetramethylaluminate) complexes perform in isoprene polymerization.

Results and discussion

Synthesis and characterization of $[(\text{Tph})_2\text{N}_3]\text{Ln}(\text{AlMe}_4)_2$ (2)

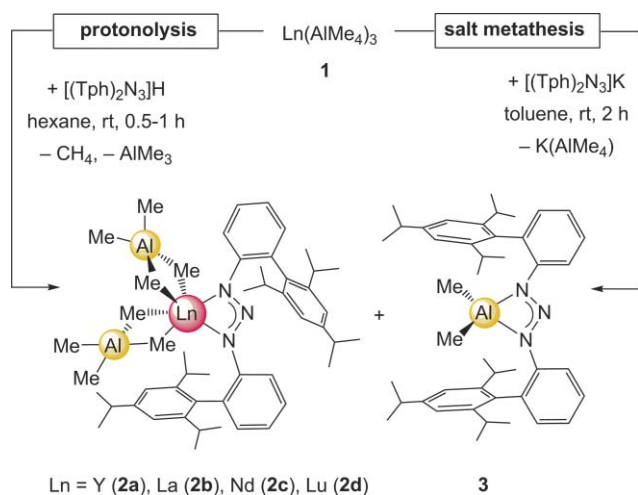
Bis(tetramethylaluminate) complexes $[(\text{Tph})_2\text{N}_3]\text{Ln}(\text{AlMe}_4)_2$ (2) (Ln = Y(a), La(b), Nd(c), Lu(d)) were prepared by applying a protonolysis protocol based on $[(\text{Tph})_2\text{N}_3]\text{H}$ and $\text{Ln}(\text{AlMe}_4)_3$ (1), or *via* a salt metathesis reaction pathway utilizing the potassium salt of the triazene proligand instead (Scheme 1). An instantaneous colour change of the reaction mixtures from light to bright yellow, or orange brown in the case of neodymium, accompanied

^aDepartment of Chemistry, University of Bergen, Allégaten 41, 5007, Bergen, Norway

^bInstitut für Anorganische und Analytische Chemie, Johannes Gutenberg-Universität Mainz, Duesbergweg 10-14, 55128, Mainz, Germany

^cInstitut für Anorganische Chemie, Universität Tübingen, Auf der Morgenstelle 18, 72076, Tübingen, Germany. E-mail: reiner.anwander@uni-tuebingen.de; Fax: +49(0)7071-29-2436; Tel: +49(0)7071-29-72069

† CCDC reference numbers 757139–757142. For crystallographic data in CIF or other electronic format see DOI: 10.1039/b925837j



Scheme 1 Synthesis of $[(\text{Tph})_2\text{N}_3]\text{Ln}(\text{AlMe}_4)_2$ (**2**) via protonolysis and salt metathesis reaction pathways.

by methane formation and $[\text{KAlMe}_4]$ precipitation, respectively, indicated coordination of the monoanionic triazenido ligand to the rare-earth metal centre. Upon removal of the solvent and the volatile byproducts (or $[\text{KAlMe}_4]$), bright yellow solids of complexes **2** were obtained, however, contaminated by the dimethylaluminium byproduct $[(\text{Tph})_2\text{N}_3]\text{AlMe}_2$ (**3**).^{18a}

Both the bis(tetramethylaluminate)s **2**, except **2b**, and the byproduct **3** are highly soluble in aromatic and aliphatic solvents, which hampers their separation. Based on the ^1H NMR spectra of the crude reaction products of the diamagnetic complexes, the approximate ratio of yttrium complex **2a** and undesired byproduct **3** could be estimated as 1 : 1, while in the case of lanthanum the ratio was slightly higher, and for lutetium a bit lower. This can be rationalized on the basis of steric effects: due to the high affinity of the triazenido ligand toward the more Lewis-acidic and harder aluminium cation the rare-earth metal centre of the sterically more crowded $\text{Lu}(\text{AlMe}_4)_3$ is less accessible. This tendency of *N*-chelating ligands to coordinate to $\text{Al}(\text{III})$ centres has been observed previously.^{14a,19,20}

In an attempt to increase the yield of complexes **2** relative to byproduct **3** the reactions were performed with two equivalents of proligand. This led to the complete (La) or almost complete (Y and Lu) disappearance of the homoleptic precursor **1**, leftovers of which were observed in the raw products from all of the 1 : 1 reactions. Unfortunately, the two-equivalent reactions also considerably increased the yield of byproduct **3**.

Through fractional crystallization we were able to collect single crystals of **2a**, **2c** and **2d** suitable for X-ray structure analysis. The yttrium (**2a**) and lutetium (**2d**) derivatives are isostructural and crystallize in the monoclinic space group $P2_1/n$, with one molecule hexane per two crystallographically independent molecules (the D and L enantiomers) of the product, while the neodymium derivative (**2c**) crystallizes without solvent molecules in the monoclinic space group $P2_1/c$. An ORTEP drawing of the yttrium complex **2a** is shown in Fig. 1, and selected bond distances and angles of complexes **2a** and **2d** are listed in Table 1. The rare-earth metal centre is six-coordinate and adopts a distorted octahedral coordination geometry. The η^2 -bonded triazenido ligand displays an asymmetrical *syn/anti* conformation with no additional metal-

π -arene interactions like those observed in the potassium complex $[(\text{Tph})_2\text{N}_3]\text{K}$ ¹⁶ or the divalent europium and ytterbium complexes $[(\text{Dmp})(\text{Tph})\text{N}_3]\text{Ln}^{\text{II}}(\text{C}_6\text{F}_5)$ ($\text{Dmp} = [2,6-(2,4,6\text{-Me}_3\text{C}_6\text{H}_2)_2\text{C}_6\text{H}_3]$, $\text{Tph} = [2-(2,4,6\text{-iPr}_3\text{C}_6\text{H}_2)\text{C}_6\text{H}_4]$, $\text{Ln} = \text{Eu}, \text{Yb}$).¹¹ The metal atoms are shifted slightly out of the N_3 plane of the ligand ($\angle\text{N6-N4-N5-Ln2}$ 8.6° (**2a**); 7.5° (**2d**)). Both $[\text{AlMe}_4]$ ligands coordinate in a η^2 fashion with one of the ligands closer to planarity than the other ($\angle\text{C55-Ln2-C56-Al4}$ -4.6° (**2a**); -4.3° (**2d**), $\angle\text{C51-Ln2-C52-Al3}$ 9.9° (**2a**); 9.7° (**2d**)). All Ln–C bond lengths are in the expected range (**2a** 2.495 Å (av); **2d** 2.451 Å (av)).^{21,22} Interestingly, the Y–C bond lengths are slightly shorter than those observed in the similar amidinate complex $[(\text{NCN}^{\text{dipp}})\text{Y}(\text{AlMe}_4)_2]$ ^{3a} (2.533 Å (av)) therefore reflecting the weaker donor character^{9,18b,c} of the triazenido compared with the amidinato ligand. Even though the triazenido ligand coordinates in an asymmetrical *syn/anti* fashion, the two Ln–N bond lengths are very similar (Y–N 2.345(3)–2.365(3) Å, Lu–N 2.296(6)–2.332(6) Å).

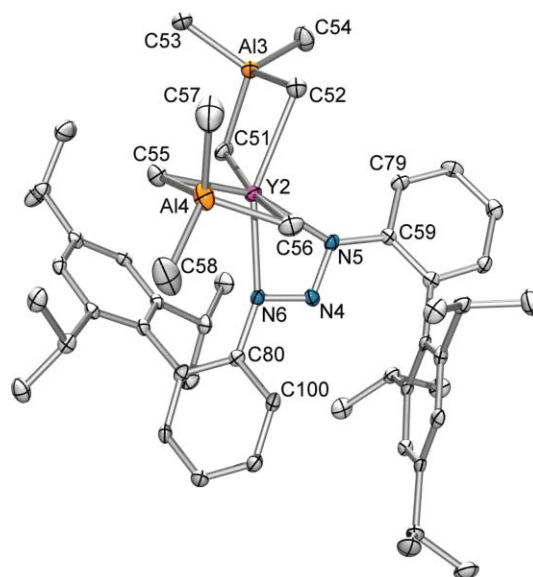


Fig. 1 Molecular structure of molecule **2** of **2a**. Atoms are represented by atomic displacement ellipsoids set at the 50% level. Hydrogen atoms and solvent are omitted for clarity.

Also in neodymium complex **2c** the η^2 -bonded triazenido ligand coordinates in an asymmetrical *syn/anti* fashion with no additional metal- π -arene interactions (Fig. 2, Table 2). However, the two $[\text{AlMe}_4]$ ligands feature distinct coordination motifs in the solid state; one of them shows the routine planar η^2 coordination ($\angle\text{C5-Nd1-C6-Al2}$ 2.5°), while the other one is bent ($\angle\text{C1-Nd1-C2-Al1}$ -37.5°). Such a bent η^2 coordination of the aluminate group will accomplish a better steric saturation of the larger neodymium metal centre. Non-planar tetraalkylaluminate coordination has been observed earlier in neodymium complexes $(\text{C}_5\text{Me}_3)\text{Nd}(\text{AlMe}_4)_2$,²³ $[\text{C}_5\text{H}_3(\text{SiMe}_3)_2]\text{Nd}(\text{AlMe}_4)_2$,¹⁵ $[\text{C}_7\text{H}_2(\text{CMe}_3)_3]\text{Nd}(\text{AlMe}_4)_2$,¹⁵ (η^2 - PC_4Me_4) $\text{Nd}(\text{AlMe}_4)_2$,¹⁷ and $[\eta^2$ - $\text{PC}_4\text{Me}_2(\text{SiMe}_3)_2]\text{Nd}(\text{AlMe}_4)_2$.¹⁷ For complex **2c**, the $\text{Nd}\cdots\text{C3}$ contact originating from this aluminate bending is significantly shorter than observed earlier (2.973(6) Å, compared to 3.088–3.326 Å), almost approaching a η^3 coordination as found in the pentaneodymium cluster $\{\text{Cp}^*_5\text{Nd}_5[(\mu\text{-Me})_3\text{AlMe}](\mu_4\text{-Cl})(\mu_3\text{-Cl})_2(\mu_2\text{-Cl})_6\}$ ($\text{Nd}\cdots\text{C}$ 2.88(2), 2.88(2), 2.78(2) Å).²⁴ As in the case

Table 1 Selected Interatomic Distances, Angles, and Dihedral Angles for [(Tph)₂N₃]Ln(AlMe₂)₂, Ln = Y (**2a**), Lu (**2d**)

	2a (Ln = Y)		2d (Ln = Lu)	
	Molecule 1	Molecule 2	Molecule 1	Molecule 2
Bond Distances/Å				
Ln1(2)–N2(5)	2.345(3)	2.358(3)	2.296(6)	2.304(6)
Ln1(2)–N3(6)	2.365(3)	2.358(3)	2.325(6)	2.332(6)
Ln1(2)⋯Al1(3)	3.044(1)	3.066(1)	2.997(3)	3.015(2)
Ln1(2)⋯Al2(4)	3.061(1)	3.052(1)	3.021(2)	3.000(2)
Ln1(2)–C1(51)	2.476(4)	2.478(4)	2.418(8)	2.440(8)
Ln1(2)–C2(52)	2.506(4)	2.518(4)	2.471(8)	2.471(8)
Ln1(2)–C5(55)	2.478(4)	2.472(4)	2.429(8)	2.427(8)
Ln1(2)–C6(56)	2.515(5)	2.512(4)	2.452(9)	2.467(8)
Ln⋯C(Ph _{syn}) (av)	4.66	4.67	4.70	4.70
Al1(3)–C1(51)	2.093(5)	2.083(4)	2.093(9)	2.079(8)
Al1(3)–C2(52)	2.075(5)	2.077(5)	2.073(8)	2.077(8)
Al1(3)–C3(53)	1.940(6)	1.961(4)	1.928(11)	1.960(8)
Al1(3)–C4(54)	1.961(6)	1.965(4)	1.956(11)	1.958(8)
Al2(4)–C5(55)	2.069(4)	2.090(5)	2.066(8)	2.089(8)
Al2(4)–C6(56)	2.076(5)	2.075(5)	2.069(8)	2.071(8)
Al2(4)–C7(57)	1.965(5)	1.956(5)	1.970(8)	1.955(10)
Al2(4)–C8(58)	1.962(5)	1.959(5)	1.960(9)	1.957(9)
N1(4)–N2(5)	1.315(4)	1.307(4)	1.322(8)	1.306(8)
N1(4)–N3(6)	1.324(4)	1.330(4)	1.326(8)	1.317(8)
Bond Angles (°)				
N2(5)–Ln1(2)–N3(6)	54.59(11)	54.58(11)	55.7(2)	55.6(2)
Ln1(2)–C1(51)–Al1(3)	83.09(15)	84.00(15)	82.9(3)	83.3(3)
Ln1(2)–C2(52)–Al1(3)	82.72(15)	83.10(15)	82.0(3)	82.6(3)
Ln1(2)–C5(55)–Al2(4)	84.12(15)	83.53(15)	84.0(3)	82.9(3)
Ln1(2)–C6(56)–Al2(4)	83.05(15)	82.80(15)	83.4(3)	82.3(3)
C1(51)–Ln1(2)–C2(52)	85.47(15)	83.92(14)	87.0(3)	85.5(3)
C1(51)–Al1(3)–C2(52)	108.43(18)	106.86(17)	107.8(3)	106.6(3)
C5(55)–Ln1(2)–C6(56)	84.04(14)	85.12(15)	85.3(3)	86.7(3)
C5(55)–Al2(4)–C6(56)	107.46(18)	108.08(18)	106.2(3)	107.7(3)
N2(5)–N1(4)–N3(6)	109.9(3)	110.2(3)	109.1(5)	111.1(6)
Dihedral Angles (°)				
N3(6)–N1(4)–N2(5)–Ln1(2)	–3.6(3)	8.6(3)	–3.2(5)	7.5(5)
N1(4)–N2(5)–C9(59)–C29(79)	–147.2(3)	153.5(3)	–146.7(6)	152.9(6)
N1(4)–N3(6)–C30(80)–C50(100)	–43.8(5)	38.9(5)	–43.7(9)	38.8(9)

of the yttrium and lutetium derivatives **2a** and **2d**, the Nd–N bond lengths are similar (2.454(4) and 2.470(4) Å).

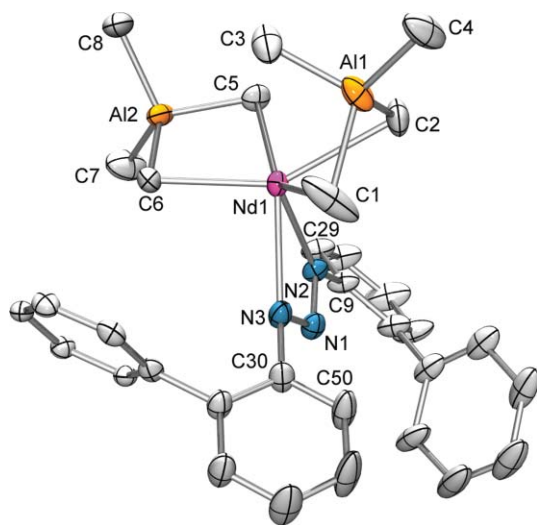


Fig. 2 Molecular structure of **2c**. Atoms are represented by atomic displacement ellipsoids set at the 50% level. Hydrogen atoms and *i*Pr-substituents are omitted for clarity.

Because of the high affinity of the triazenido ligand toward aluminium, and formation of the byproduct **3**, clean NMR spectra of products **2** were difficult to obtain. Even NMR spectra of crystallized compounds **2** (confirmed by X-ray structural and elemental analysis) revealed a product/byproduct mixture, which implies that formation of byproduct **3** is favourable over time. Overlapping peaks in the ¹H NMR spectra were therefore a problem for the assignment of some of the peaks and integral values. The ¹H NMR spectra of complexes **2a** and **2b** in C₆D₆, at ambient temperature, are indicative of more symmetric ligand environments than found in the solid state, which implies that the aromatic substituents of the coordinated ligand are highly flexible in solution. The methine protons of the isopropyl groups give three doublets, two for the *o*-positioned isopropyl groups (**2a** 1.05, 1.15 ppm; **2b** 1.06, 1.15 ppm) and one for those in *p*-position (**2a** 1.30 ppm; **2b** 1.32 ppm), each counting twelve protons. For comparison, the proligand shows a much less symmetric environment in C₆D₆ giving six different doublets, one for each isopropyl group. Correspondingly, the methine protons give two septets with a ratio of 2:1, which can be assigned to those in *o*- and *p*-position, respectively (**2a** 2.74, 2.88 ppm; **2b** 2.78, 2.91 ppm), while the proligand shows three different methine signals. Also the [AlMe₂] moieties of complex **2a** and **2b** show high fluxionality in solution. Only one signal is observed for the aluminium bound methyl groups at 25 °C (**2a** –0.24 ppm; **2b** –0.15 ppm), and

Table 2 Selected Interatomic Distances, Angles, and Dihedral Angles for [(Tph)₂N₃]Nd(AlMe₄)₂ (**2c**)

	2c
Bond Distances (Å)	
Nd1–N2	2.454(4)
Nd1–N3	2.470(4)
Nd1...Al1	2.9180(17)
Nd1...Al2	3.1663(16)
Nd1–C1	2.713(6)
Nd1–C2	2.708(6)
Nd1...C3	2.973(6)
Nd1–C5	2.640(5)
Nd1–C6	2.562(5)
Nd1...C(Ph _{syn}) (av)	5.035
Al1–C1	2.060(7)
Al1–C2	2.048(7)
Al1–C3	1.987(7)
Al1–C4	1.949(6)
Al2–C5	2.055(6)
Al2–C6	2.085(6)
Al2–C7	1.964(7)
Al2–C8	1.976(6)
N1–N2	1.325(6)
N1–N3	1.304(6)
Bond Angles (°)	
N2–Ln1–N3	52.20(13)
Nd1–C1–Al1	74.0(2)
Nd1–C2–Al1	74.25(18)
Nd1–C3–Al1	68.81(18)
Nd1–C5–Al2	83.83(18)
Nd1–C6–Al2	85.24(19)
C1–Ln1–C2	72.3(2)
C1–Al1–C2	102.2(3)
C1–Ln1–C3	68.2(3)
C1–Al1–C3	104.3(4)
C2–Ln1–C3	69.78(18)
C2–Al1–C3	107.6(3)
C5–Ln1–C6	81.14(18)
C5–Al2–C6	109.6(2)
N2–N1–N3	110.9(4)
Dihedral Angles (°)	
N3–N1–N2–Nd1	13.2(4)
N1–N2–C9–C29	144.0(5)
N1–N3–C30–C50	50.2(7)

in the case of the yttrium derivative a characteristic splitting of the peak is observed due to coupling to the yttrium metal centre ($^2J_{YH} = 2.3$ Hz). Variable temperature ^1H NMR studies of complex **2a** in toluene-*d*₆ did not show any decoalescence for the signals of these methyl groups at temperatures down to -80 °C ($\Delta\nu_{1/2} \approx 8$ Hz at -80 °C), similar to homoleptic precursor **1a**.²¹ This implies rapid exchange between bridging and terminal methyl groups even at low temperatures. Furthermore, there is no splitting of the peaks corresponding to the isopropyl groups of the ancillary ligand at -80 °C. The ligand environment in complex **2d** is slightly less symmetric in C₆D₆, most likely due to the high steric crowding around the small lutetium metal centre. However, as mentioned earlier, no additional metal- π -arene interactions are observed in the solid-state structure. For complex **2d** five different methyl signals (1.31, 1.27, 1.15, 1.12, 1.05 ppm) are observed for the isopropyl groups, assignable to two *p*-positioned, two *o*-positioned, and two equivalent *o*-positioned isopropyl groups, respectively. As for the proligand, three methine signals are observed (2.71, 2.84, 2.87 ppm). The [AlMe₄] moieties of complex **2d** show enhanced fluxionality even at temperatures down to -80 °C ($\Delta\nu_{1/2} \approx 8$ Hz at -80 °C).

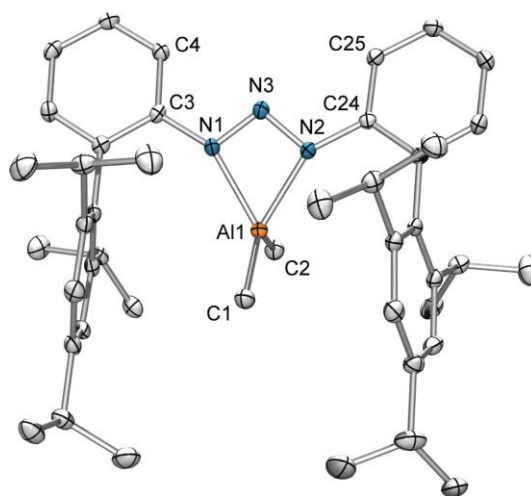
Table 3 Selected Interatomic Distances, Angles, and Dihedral Angles for [(Tph)₂N₃]AlMe₂ (**3**)

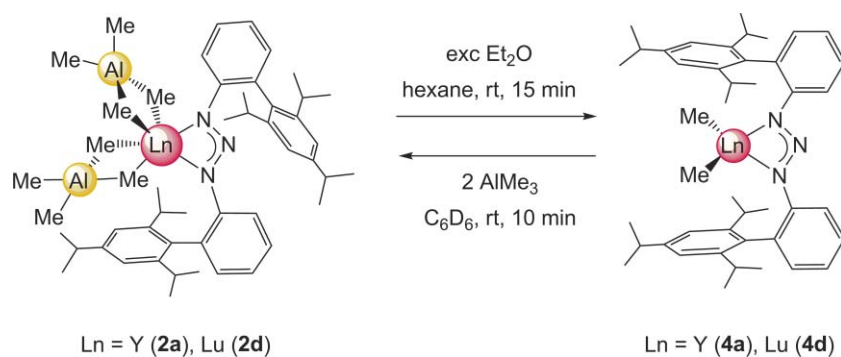
	3
Bond Distances (Å)	
Al1–C1	1.933 (2)
Al1–C2	1.950 (2)
Al1–N1	1.983(1)
Al1–N2	1.975(1)
Al1...C(Ph) (av)	4.193
N1–N3	1.311(2)
N2–N3	1.323(2)
Bond Angles (°)	
C1–Al1–C2	122.68(7)
N1–Al1–N2	64.49(5)
N1–N3–N2	106.6(1)
Dihedral Angles (°)	
N1–N3–N2–Al1	7.2(1)
N3–N1–C3–C4	19.8(2)
N3–N2–C24–C25	-16.9(2)

The presence of byproduct **3** also hampered the interpretation of the ^{13}C NMR spectra. For yttrium complex **2a** the assignment of all product peaks was possible, even though byproduct **3** gives the strongest peaks. The [AlMe₄] signal at 3.5 ppm revealed a ^{13}C - ^{89}Y scalar coupling ($^1J_{YC} = 4.6$ Hz). As opposed to all other complexes, the lanthanum derivative **2b** is less soluble in aliphatic hydrocarbons than byproduct **3**, facilitating its isolation and purification. Attempts to dissolve these purified samples in C₆D₆ to measure ^{13}C NMR spectra resulted in the same type of ligand scrambling and, despite the considerable higher concentration of complex **2b**, only a few peaks could be assigned definitely.

Synthesis and characterization of [(Tph)₂N₃]AlMe₂ (**3**)

Byproduct **3** was independently synthesized in quantitative yield *via* addition of AlMe₃ to a hexane solution of proligand [(Tph)₂N₃]H. Instant colour change of the reaction mixture from light to bright yellow and methane formation indicated the formation of compound [(Tph)₂N₃]AlMe₂ (**3**). Crystallization of complex **3** from a hexane solution produced single crystals suitable for X-ray structure analysis. **3** crystallizes in the monoclinic space

**Fig. 3** Molecular structure of **3**. Atoms are represented by atomic displacement ellipsoids set at the 50% level. Hydrogen atoms are omitted for clarity.



Scheme 2 Synthesis of $[(\text{Tph})_2\text{N}_3]\text{LnMe}_2$ (**4**) via donor-induced cleavage of $[(\text{Tph})_2\text{N}_3]\text{Ln}(\text{AlMe}_4)_2$.

group $P2_1/n$ and adopts a distorted tetrahedral geometry (Fig. 3, Table 3). In contrast to the rare-earth metal complexes **2**, the η^2 -coordinated triazenido ligand features an almost symmetric *syn/syn* configuration. Additional π -interaction between the metal centre and the arene rings of the ligand are not observed ($\text{Al}-\text{C}_{\text{ph}}$ 4.193 Å (av)). The aluminium atom is shifted slightly out of the N_3 plane of the ligand ($\angle\text{N1}-\text{N3}-\text{N2}-\text{Al1}$ 7.2°), and the Al–C bond lengths ($\text{Al1}-\text{C1}$ 1.933(2) Å, $\text{Al1}-\text{C2}$ 1.950(2) Å) are similar to those observed in structurally related dimethyl-aluminium amidinate ($[\text{MeC}(\text{NSiMe}_3)_2]\text{AlMe}_2$ ²⁵ (1.942 Å (av)), $[\text{MeC}(\text{NCy})_2]\text{AlMe}_2$ ²⁶ (1.958 Å (av)), $[\text{tBuC}(\text{NCy})_2]\text{AlMe}_2$ ²⁶ (1.954 Å (av)) and β -diketiminate ($[(2,6\text{-}i\text{Pr}_2\text{C}_6\text{H}_3)_2(\text{nacnac})]\text{AlMe}_2$ ^{27,28} (1.967 Å (av)), $[(\text{HC}(\text{CMe}_2)(N\text{-}p\text{-tolyl})_2]\text{AlMe}_2$ ²⁷ (1.958 Å (av)), $[(\text{HC}(\text{CMe}_2)(\text{NC}_6\text{F}_5)_2]\text{AlMe}_2$ ²⁹ (1.952 Å (av)) complexes.

As expected, the ¹H NMR spectrum of the aluminium complex **3** in C_6D_6 shows a quite symmetric ligand environment. As for complexes **2a** and **2b**, three doublets are observed for the methyl protons of the isopropyl groups (*o*-position: 1.06, 1.18 ppm; *p*-position: 1.29 ppm) and two septets in a ratio of 2 : 1, accounting for *o*- (2.71 ppm) and *p*-positioned (2.85 ppm) methine protons, respectively.

Attempted synthesis of $\{[(\text{Tph})_2\text{N}_3]\text{LnMe}_2\}$

Attempts were made to synthesize dimethyl complexes of the formula $[(\text{Tph})_2\text{N}_3]\text{LnMe}_2$ (**4**) via donor-induced cleavage of complexes **2a** and **2d** (Scheme 2), as described earlier for the corresponding pentamethylcyclopentadienyl complexes.³⁰ Addition of an excess of Et_2O to a hexane solution of the respective complexes **2** (contaminated with byproduct **3**) did not result in any visual changes. The mixture remained a bright yellow solution. From the ¹H NMR of the product mixture one could, however, observe the disappearance of the $[\text{AlMe}_4]$ peak. Unfortunately, the concentration of putative product **4** was too low for any peaks to be assigned, due to ligand redistribution and extensive formation of **3**. Upon addition of two equivalents of AlMe_3 to this mixture the $[\text{AlMe}_4]$ peak reappeared, which might indicate a reversible formation of dimethyl complexes **4** from **2**. Furthermore, the redistribution of complexes **2** in solution, to give mixtures of **2** and **3**, is always accompanied by formation of some of the homoleptic starting material $\text{Ln}(\text{AlMe}_4)_3$ (**1**). Donor-induced cleavage of complexes **1** with Et_2O should produce insoluble $[\text{LnMe}_3]_n$ derivatives,³¹ precipitation of which, however, did not occur in the present cleavage reactions. This would be in favour

of the formation of soluble dimethyl complexes **4**. Attempts to crystallize such dimethyl derivatives have so far only resulted in the isolation of byproduct **3**.

Polymerization of isoprene

As an extension of our tetramethylaluminate-based postmetallocene library¹⁵ rare-earth metal complexes **2** were initially examined as precatalysts for the polymerization of isoprene. Given the intrinsic ligand scrambling and redistribution reactions in solution, this turned out to be a challenging task. In addition to the rare-earth metal complexes **2** under investigation, we had to consider additional active/co-influencing components originating from residual homoleptic precursors **1** and byproduct **3**. In order to investigate the effect of these side-products, pure samples of these compounds were also tested as precatalysts. Significant amounts of isolated complexes **2** were only obtained for the derivatives of the larger metal centres lanthanum and neodymium, by exploiting distinct solubility behaviour and fractional crystallization, respectively. Accordingly, isolated samples of **2b** and **2c** were used, in addition to *in situ* formed catalyst mixtures. For yttrium derivative **2a**, representing the smaller rare-earth metal centres, only the *in situ* formed complex was tested as a precatalyst. To reduce the amount of homoleptic rare-earth metal complexes **1** present in the *in situ* formed catalyst mixtures of complexes **2**, 1 : 2 ratios of precursors **1** and the proligand were employed. $[\text{Ph}_3\text{C}][\text{B}(\text{C}_6\text{F}_5)_4]$ (**A**), $[\text{PhNMe}_2\text{H}][\text{B}(\text{C}_6\text{F}_5)_4]$ (**B**), and $\text{B}(\text{C}_6\text{F}_5)_3$ (**C**) were used as activators. The polymerization results are summarized in Table 4.

The aluminium compound **3** did not polymerize isoprene, neither without nor with addition of borane or borate activators (not shown in Table 4).³² Homoleptic complexes **1** did, however, show good to excellent activity in the polymerization of isoprene upon activation with $\text{B}(\text{C}_6\text{F}_5)_3$ (**C**) or $[\text{Ph}_3\text{C}][\text{B}(\text{C}_6\text{F}_5)_4]$ (**A**)/ $[\text{PhNMe}_2\text{H}][\text{B}(\text{C}_6\text{F}_5)_4]$ (**B**), respectively (Table 4, runs 1–9). The stereoselectivities produced by these binary catalyst mixtures are pretty low, with similar *cis*-1,4 and *trans*-1,4 contents for complexes **1b** and **1c** (Table 4, runs 4-8), and a slightly higher *cis*-1,4 content for complex **1a** (Table 4, runs 1–3). Noteworthy exception is catalyst system $\text{Nd}(\text{AlMe}_4)_3$ (**1c**)/ $\text{B}(\text{C}_6\text{F}_5)_3$ (**C**) revealing excellent activity with quantitative yield and 87% *cis*-1,4 selectivity (Table 4, run 9). Runs 2 and 8 involving catalysts $\text{Y}(\text{AlMe}_4)_3$ (**1a**)/ $[\text{PhNMe}_2\text{H}][\text{B}(\text{C}_6\text{F}_5)_4]$ (**B**) and $\text{Nd}(\text{AlMe}_4)_3$ (**1c**)/ $[\text{PhNMe}_2\text{H}][\text{B}(\text{C}_6\text{F}_5)_4]$ (**B**) are in accordance with previously reported performances of these binary systems, nicely demonstrating the reproducibility of such polymerization data.^{33,34}

Table 4 Polymerization of isoprene by precatalysts [(Tph)₂N₃]Ln(AlMe₄)₂ (**2**)³⁵

Entry ^a	Precatalyst	Cocatalyst ^c	Yield (%)	Structure ^d			$M_n^e (\times 10^5)$	M_w/M_n^e	Efficiency ^f (%)
				<i>trans</i> -1,4-	<i>cis</i> -1,4-	3,4-			
1	Y(AlMe ₄) ₃ (1a)	A	>99	23.6	69.1	7.3	0.9	2.09	75
2	Y(AlMe ₄) ₃ (1a)	B	>99	21.2	68.8	10.1	1.1	1.93	62
3	Y(AlMe ₄) ₃ (1a)	C	56.2	35.1	62.5	2.4	1.2	2.03	32
4	La(AlMe ₄) ₃ (1b)	A	>99	51.4	46.3	2.3	0.5	1.29	138
5	La(AlMe ₄) ₃ (1b)	B	>99	46.8	49.8	3.4	0.6	1.23	120
6	La(AlMe ₄) ₃ (1b)	C	80.0	59.5	39.1	1.4	3.3	1.18	16
7	Nd(AlMe ₄) ₃ (1c)	A	>99	44.0	51.0	5.1	0.5	1.89	147
8	Nd(AlMe ₄) ₃ (1c)	B	>99	44.9	50.8	4.3	0.4	1.77	158
9	Nd(AlMe ₄) ₃ (1c)	C	>99	10.1	86.6	3.4	1.6	1.65	42
10	[(Tph) ₂ N ₃]Y(AlMe ₄) ₂ (2a)	—	—	—	—	—	—	—	—
11	[(Tph) ₂ N ₃]Y(AlMe ₄) ₂ (2a)	A	>99	41.0	49.6	9.4	0.8	1.41	88
12	[(Tph) ₂ N ₃]Y(AlMe ₄) ₂ (2a)	B	>99	31.4	57.5	11.1	0.6	1.52	123
13	[(Tph) ₂ N ₃]Y(AlMe ₄) ₂ (2a)	C	—	—	—	—	—	—	—
14	[(Tph) ₂ N ₃]La(AlMe ₄) ₂ (2b)	—	—	—	—	—	—	—	—
15	[(Tph) ₂ N ₃]La(AlMe ₄) ₂ (2b)	A	>99	74.2	23.1	2.7	0.6	1.35	112
16	[(Tph) ₂ N ₃]La(AlMe ₄) ₂ (2b)	B	>99	82.6	14.9	2.5	0.5	1.13	125
17	[(Tph) ₂ N ₃]La(AlMe ₄) ₂ (2b)	C	10.3	89.4	8.6	2.0	0.3	2.02	23
18 ^b	[(Tph) ₂ N ₃]La(AlMe ₄) ₂ (2b)	A	>99	81.0	16.1	3.0	0.6	1.28	108
19 ^b	[(Tph) ₂ N ₃]La(AlMe ₄) ₂ (2b)	B	>99	91.7	6.3	2.1	0.7	1.30	95
20 ^b	[(Tph) ₂ N ₃]La(AlMe ₄) ₂ (2b)	C	40.2	89.2	8.8	2.0	0.9	2.04	33
21	[(Tph) ₂ N ₃]Nd(AlMe ₄) ₂ (2c)	—	—	—	—	—	—	—	—
22	[(Tph) ₂ N ₃]Nd(AlMe ₄) ₂ (2c)	A	>99	81.2	16.4	2.4	0.5	1.40	135
23	[(Tph) ₂ N ₃]Nd(AlMe ₄) ₂ (2c)	B	>99	76.0	21.7	2.3	0.5	1.42	143
24	[(Tph) ₂ N ₃]Nd(AlMe ₄) ₂ (2c)	C	84.9	61.3	35.6	3.2	1.3	2.93 ^g	26
25 ^b	[(Tph) ₂ N ₃]Nd(AlMe ₄) ₂ (2c)	A	>99	90.0	8.0	2.0	0.6	1.51	110
26 ^b	[(Tph) ₂ N ₃]Nd(AlMe ₄) ₂ (2c)	B	>99	89.4	8.6	2.0	0.5	1.36	133
27 ^b	[(Tph) ₂ N ₃]Nd(AlMe ₄) ₂ (2c)	C	2.2	28.7	67.2	4.1	1.4	3.63 ^g	<1

^a Conditions: 0.02 mmol precatalyst formed *in situ*, [Ln]/[cocat] = 1 : 1, 8 mL toluene, 20 mmol isoprene, 24 h, ambient temperature. ^b Isolated sample used as precatalyst. ^c Cocatalyst: **A** = [Ph₃C][B(C₆F₅)₄], **B** = [PhNMe₂H][B(C₆F₅)₄], **C** = B(C₆F₅)₃; the catalyst was preformed for 30 min at ambient temperature.

^d Determined by ¹H and ¹³C NMR spectroscopy in CDCl₃. ^e Determined by means of size-exclusion chromatography (SEC) against polystyrene standards.

^f Initiation efficiency = $M_n(\text{calculated})/M_n(\text{measured})$. ^g Bimodal distributions with significantly different M_n values were obtained for catalyst systems **2c/C** (run 24, major part (72%): $M_n = 1.0 \times 10^5$, $M_w/M_n = 1.07$; run 24, minor part (28%): $M_n = 7.4 \times 10^5$, $M_w/M_n = 1.44$; run 27, major part (51%): $M_n = 4.9 \times 10^5$, $M_w/M_n = 1.66$; run 27, minor part (49%): $M_n = 0.1 \times 10^5$, $M_w/M_n = 1.81$).

All precatalysts **2** showed extremely high activities upon activation with [Ph₃C][B(C₆F₅)₄] (**A**) or [PhNMe₂H][B(C₆F₅)₄] (**B**), independent on the size of the metal cation. The activation capability of B(C₆F₅)₃ (**C**) seems to be generally low and depends considerably on the metal cation size, since the yttrium derivative **2a** did not give any polyisoprene upon addition of B(C₆F₅)₃ (Table 4, run 13). For all activations of complexes **2**, a colour change from bright yellow to orange was observed independent on the boron activator.

Due to the interference of homoleptic complexes **1** in solutions of precatalysts **2**, it is difficult to discuss the effect of the rare-earth metal on the stereoselectivity of the polymerization reactions in detail. One clearly sees a different performance of the smaller yttrium compared to the larger neodymium and lanthanum derivatives; while the latter precatalysts **2b** and **2c** display relatively high *trans*-1,4 selectivities (Table 4, runs 15–20 and 22–27), yttrium complex **2a** produces slightly higher *cis*-1,4 contents, and also a slightly higher 3,4 content (Table 4, runs 11 and 12). This could be a metal size effect, but at the same time the yttrium system implies a higher concentration of homoleptic complex **1a**, which will cause a shift toward higher *cis*-1,4 contents of the polymers (Table 4, runs 1–3).

Having a closer look at the polymerization reactions performed with precatalyst **2b**, there seems to be negligible interference of homoleptic complex **1b**, independent on which activator is used.

All catalyst mixtures produce polyisoprene with high *trans*-1,4 content, comparable M_n and relatively narrow molecular weight distributions (Table 4, runs 15–20), with the highest *trans*-1,4 selectivity of 91.7% obtained with activator [PhNMe₂H][B(C₆F₅)₄] (**B**) (Table 4, run 19). The performance of the neodymium derivative **2c** seems to be considerably affected by homoleptic complex **1c** present in the system. This is particularly evident for the B(C₆F₅)₃ (**C**)-based initiators (Table 4, runs 24 and 27), which show a relatively high *cis*-1,4 content and pronounced bimodal molecular weight distributions. Except for these latter initiators, all catalyst systems tested revealed relatively low molecular weights, which could be explained by polymer chain-transfer promoted by the various organoaluminium species present in solution.³⁶ The molecular weight distributions produced by the initiators **2/A** and **2/B** are smaller than 1.5.

Table 5 summarizes important polymerization data of bis(alkyl) rare-earth metal complexes supported by monoanionic *N*-coordinating ancillary ligands including amidinato, pyrrolido, aminopyridinato and other types of substituted amido ligands (Chart 1).^{3a,5a,7a,c-f,37} It is very clear that the polymerization performance and in particular the stereoselectivity is crucially affected by the *N*-coordinating ancillary ligands. In 2007 Hou *et al.* reported on bis(phosphinophenyl)amido (PNP) supported rare-earth metal bis(alkyls) **I** that promote the living *cis*-1,4-polymerization of isoprene upon cationization with borate [PhNMe₂H][B(C₆F₅)₄] (**B**).³⁷

Table 5 Previously reported results for isoprene polymerization by bis(alkyl) rare-earth metal complexes containing *N*-coordinating ancillary ligands

Precatalyst	Cocatalyst ^a	Time	<i>T</i> /°C	Yield (%)	Structure			<i>M_n</i> (× 10 ⁵)	<i>M_w</i> / <i>M_n</i>	Ref.
					3,4-	<i>cis</i> -1,4-	<i>trans</i> -1,4-			
[(2-(Ph ₂ P)C ₆ H ₄) ₂ N]Y(CH ₂ SiMe ₃) ₂ (thf) I	B	3 h	0	100	0.4	99.6	—	1.3	1.06	37
[(2,6- <i>i</i> Pr ₂ C ₆ H ₃ N) ₂ PhC]Y(<i>o</i> -CH ₂ C ₆ H ₄ NMe ₂) ₂ II	A	20 min	-20	100	99.5	0.5	—	1.7	1.4	3a
[(2,6- <i>i</i> Pr ₂ C ₆ H ₃ N) ₂ PhC]Y(<i>o</i> -CH ₂ C ₆ H ₄ NMe ₂) ₂ II	A /AlMe ₃	16 h	-20	100	1	>98	<1	4.0	1.7	3a
{(2,6- <i>i</i> Pr ₂ C ₆ H ₃)}[6-(2,4,6- <i>i</i> Pr ₃ C ₆ H ₂)C ₅ H ₃ -2-N]N]Sc(CH ₂ Ph) ₂ (thf) III	A	20 h	20	97	95	5	—	1.3	1.68	5a
{(2,6- <i>i</i> Pr ₂ C ₆ H ₃)}[6-(2,4,6- <i>i</i> Pr ₃ C ₆ H ₂)C ₅ H ₃ -2-N]N]Sc(CH ₂ Ph) ₂ (thf) III	B /AlMe ₃	20 h	20	96	10	90	—	0.7	4.51	5a
{2-[(<i>N</i> -2,6-Me ₂ C ₆ H ₃)N=CH]-C ₄ H ₃ N}Sc(CH ₂ SiMe ₃) ₂ (thf) IV	A /AlEt ₃	1 min	20	100	9.0	76.7	14.3	1.0	1.55	7e
{[2-(Me ₂ NCH ₂)-C ₄ H ₃ N]Y(CH ₂ SiMe ₃) ₂ } V	A /AlEt ₃	5 h	20	99	14.4	15.2	70.4	0.1	1.37	7e
[(<i>N</i> -2,4,6-Me ₃ C ₆ H ₂)NPPh ₂ N(Ph)]-Sc(CH ₂ SiMe ₃) ₂ (thf) VI	B /Al <i>i</i> Bu ₃	2 h	-40	97	94.7	—	5.3 ^b	9.9	1.55	7c
{7-[(<i>N</i> -2,6- <i>i</i> Pr ₂ C ₆ H ₃)N=CH]-C ₈ H ₃ N}Sc(CH ₂ SiMe ₃) ₂ (thf) VII	A /Al <i>i</i> Bu ₃	5 min	20	96	9.1	87.7	3.2	4.9	1.56	7d
[(<i>N</i> -2-EtC ₆ H ₄)NPPh ₂ N(<i>N</i> -2,6- <i>i</i> Pr ₂ C ₆ H ₃)]Sc(CH ₂ SiMe ₃) ₂ (thf) VIII	A /Al <i>i</i> Bu ₃	6 h	-20	81	99.4	0.6	—	1.5	1.5	7a
[2,6- <i>i</i> Pr ₂ C ₆ H ₃ N(SiMe ₃) ₂]Lu(CH ₂ SiMe ₃) ₂ (thf) IX	A	5 min	25	100	70	—	30 ^b	0.3	1.12	7f

^a **A** = [Ph₃C][B(C₆F₅)₄], **B** = [PhNMe₂H][B(C₆F₅)₄]. ^b *cis*-1,4 : *trans*-1,4 ratio not specified.

One year later, the same group demonstrated that the initiator mono(amidinate) bis(aminobenzyl) yttrium (**II**)/[Ph₃C][B(C₆F₅)₄] (**A**) exhibits high 3,4-stereoselectivity, a selectivity that is totally switched to *cis*-1,4 upon addition of AlMe₃ involving the formation of the corresponding bis(tetramethylaluminate) complex.^{3a} More recently, Kempe *et al.* described the same type of stereoselectivity switch when adding different alkylaluminium compounds to the bis(alkyl) scandium aminopyridinate complex **III**.^{5a} Cui *et al.* also reported on several bis(alkyl) rare-earth metal complexes (**IV-VIII**) containing different types of monoanionic *N*-coordinating ancillary ligands, and their effect in isoprene polymerization.^{7a,c-e} It was concluded that 3,4-selectivity is favoured in the case of sterically oversaturated metal centres, as evidenced for the smallest metal centre scandium in **VIII** showing the highest 3,4-selectivities, even in the presence of alkylaluminium cocatalysts. However, for initiators with sterically less saturated metal centres the addition of alkylaluminium cocatalysts results in the same *cis*-1,4-selectivity switch as reported by Hou and Kempe, suggesting the formation of

tetraalkylaluminate rare-earth metal complexes as active species in these polymerizations. The dinuclear pyrrolido supported yttrium bis(alkyl), [(2-(Me₂NCH₂)-C₄H₃N)Y(CH₂SiMe₃)₂] (**V**)^{7e} is a rare example, which gave a high *trans*-1,4 selectivity. This was argued to be a result of the special spatial environment around the metal centre. The beneficial effect of *N*-chelating ancillary ligands for achieving high stereoselectivities is evident from the mediocre performance of complex **IX**.^{7f} Importantly, for the triazenide complexes **2** under study, it is the combination of a highly flexible [NNN] ligand with large Ln(III) centres which favours *trans*-1,4 selectivity. This is in agreement with the polymerization performance of half-sandwich bis(tetramethylaluminate) complexes.¹⁵

Conclusions

Homoleptic complexes Ln(AlMe₃)₃ can be utilized in both protonolysis and salt metathesis reactions for the synthesis of triazenide bis(tetramethylaluminate) postmetallocene-type

complexes. The triazenido ligand $[(\text{Tph})_2\text{N}_3]^-$ ($\text{Tph} = [2-(2,4,6\text{-}i\text{Pr}_3\text{C}_6\text{H}_2)\text{C}_6\text{H}_4]$) proves to be a versatile ancillary ligand giving access to complexes $[(\text{Tph})_2\text{N}_3]\text{Ln}(\text{AlMe}_4)_2$ of both the smaller (Y and Lu), and larger rare-earth metals (Nd and La). However, competition of the more Lewis-acidic harder aluminium cation for the triazenido ligand gives product mixtures. Complexes $[(\text{Tph})_2\text{N}_3]\text{Ln}(\text{AlMe}_4)_2$ are active in the polymerization of isoprene, their performance being governed by the following factors: a) ligand redistribution in solution to give $\text{Ln}(\text{AlMe}_4)_3$ and $[\text{NNN}]\text{AlMe}_2$ produces additional active sites, interference being most effective for yttrium or cocatalyst C; b) large Ln(III) metal centres reveal high *trans*-1,4 selectivities (91.7% for $[(\text{Tph})_2\text{N}_3]\text{La}(\text{AlMe}_4)_2/[\text{PhNMe}_2\text{H}][\text{B}(\text{C}_6\text{F}_5)_4]$); c) relatively low molecular weights suggest polymer chain transfer *via* organoaluminium species. The binary system $\text{Nd}(\text{AlMe}_4)_3/\text{B}(\text{C}_6\text{F}_5)_3$ revealed also excellent activity with 87% *cis*-1,4 selectivity.

A more general message from this polymerization study is that rare-earth metal alkyl complexes carrying *N*-coordinating ligands are especially prone to ligand redistribution reactions in the presence of (small) organoaluminium reagents such as AlMe_3 and AlEt_3 . This will involve the formation of homoleptic Ln(III) tetraalkylaluminate species, which might drastically affect the polymerization performance.

Experimental

General considerations

All operations were performed with rigorous exclusion of air and water, using standard *Schlenk*, high-vacuum, and glovebox techniques (MBraun MBLab; <1 ppm O_2 , <1 ppm H_2O). Hexane, toluene and diethyl ether were purified by using *Grubbs* columns (MBraun SPS, solvent purification system) and stored in a glovebox. C_6D_6 and toluene- d_8 were obtained from *Aldrich*, degassed, dried over Na for 24 h, and filtered. AlMe_3 was purchased from *Aldrich* and used as received. Homoleptic $\text{Ln}(\text{AlMe}_4)_3$ (**1**) (Ln = Y, La, Nd, Lu) were prepared according to literature methods.^{21,22} $[(\text{Tph})_2\text{N}_3]\text{H}$ ($\text{Tph} = [2-(2,4,6\text{-}i\text{Pr}_3\text{C}_6\text{H}_2)\text{C}_6\text{H}_4]$) was synthesized as described earlier,¹⁶ and $[(\text{Tph})_2\text{N}_3]\text{K}$ by reacting the protonated ligand with $\text{K}[\text{N}(\text{SiMe}_3)_2]$. The NMR spectra of air and moisture sensitive compounds were recorded by using *J. Young* valve NMR tubes at 25 °C on a *Bruker* DMX-400 Avance (^1H : 400.13 Hz; ^{13}C : 100.61 MHz), a *Bruker*-BIOSPIN-AV500 (5 mm BBO, ^1H : 500.13 Hz; ^{13}C : 125.77 MHz), and a *Bruker*-BIOSPIN-AV600 (5 mm cryo probe, ^1H : 600.13 MHz; ^{13}C : 150.91 MHz). ^1H and ^{13}C shifts are referenced to internal solvent resonances and reported in *parts per million* relative to TMS. IR spectra were recorded on a *NICOLET Impact 410 FTIR* spectrometer as Nujol mulls sandwiched between CsI plates. Elemental analyses were performed on an *Elementar Vario EL III*. The molar masses (M_w/M_n) of the polymers were determined by size-exclusion chromatography (SEC). Sample solutions (1.0 mg polymer per mL THF) were filtered through a 0.2 μm syringe filter prior to injection. SEC was performed with a pump supplied by Viscotek (GPCmax VE 2001), employing ViscogEL columns. Signals were detected by means of a triple detection array (TDA 302) and calibrated against polystyrene standards ($M_w/M_n < 1.15$). The flowrate was set to 1.0 mL min^{-1} . The microstructure of the polyisoprenes was examined by means of ^1H and ^{13}C NMR

experiments on the AV500 and AV600 spectrometers at ambient temperature, using CDCl_3 as a solvent.

General procedure for the synthesis of $[(\text{Tph})_2\text{N}_3]\text{Ln}(\text{AlMe}_4)_2$ (**2**) *via* protonolysis

In a glovebox, a stirred suspension of $[(\text{Tph})_2\text{N}_3]\text{H}$ in 3 mL of hexane was added dropwise to a solution of $\text{Ln}(\text{AlMe}_4)_3$ (**1**) dissolved in 3 mL of hexane. Instant gas formation was observed, and the mixture turned from a light yellow suspension into a bright yellow, clear solution. The reaction mixture was stirred another 0.5–1 h at ambient temperature, and then dried under vacuum to yield yellow powdery solids of **2** and the byproduct **3**.

General procedure for the synthesis of $[(\text{Tph})_2\text{N}_3]\text{Ln}(\text{AlMe}_4)_2$ (**2**) *via* salt metathesis

In a glovebox, a stirred suspension of $[(\text{Tph})_2\text{N}_3]\text{K}$ in 3 mL of toluene was added dropwise to a solution of $\text{Ln}(\text{AlMe}_4)_3$ (**1**) dissolved in 3 mL of toluene. Instantaneously, the mixture turned from a yellow suspension into a clearer and more orange solution. Then it turned yellow again and gave a new suspension. The reaction mixture was stirred for another 2 h at ambient temperature. After centrifugation, the residue was washed several times with toluene and then the solution fractions combined and dried under vacuum to yield yellow powdery solids of **2** and the byproduct **3**.

The salt metathesis reactions gave approximately the same yields as the protonolysis reactions, but a slight contamination of remaining $[\text{KAlMe}_4]$ made the latter more favourable.

$[(\text{Tph})_2\text{N}_3]\text{Y}(\text{AlMe}_4)_2$ (**2a**)

Following the protonolysis procedure described above, $\text{Y}(\text{AlMe}_4)_3$ (**1a**, 57 mg, 0.16 mmol) and $[(\text{Tph})_2\text{N}_3]\text{H}$ (99 mg, 0.16 mmol) yielded **2a**, contaminated by **3**, as a powdery yellow solid (140 mg, 45%, based on ^1H NMR). Salt metathesis gave a reaction yield of 44%. Crystallization from hexane at –30 °C afforded yellow single crystals of **2a** suitable for X-ray diffraction analysis. IR (Nujol, cm^{-1}): 1610 w, 1574 w, 1460 vs (Nujol), 1378 vs (Nujol), 1323 m, 1284 s, 1197 m, 1103 w, 1057 w, 1000 w, 943 w, 881 w, 757 m, 721 m, 705 m, 581 w, 524 w cm^{-1} . ^1H NMR (600 MHz, C_6D_6 , 25 °C): $\delta = 7.21$ (s, 4 H, *m*-Trip), 7.13–7.18 (m, 2 H, ar), 7.11 (d, $^3J_{\text{HH}} = 7.4$ Hz, 2 H, ar), 6.95 (t, $^3J_{\text{HH}} = 7.4$ Hz, 2 H, ar), 6.92 (d, $^3J_{\text{HH}} = 8.0$ Hz, 2 H, ar), 2.88 (sep, $^3J_{\text{HH}} = 6.8$ Hz, 2 H, *p*- $\text{CH}(\text{CH}_3)_2$), 2.74 (sep, $^3J_{\text{HH}} = 6.8$ Hz, 4 H, *o*- $\text{CH}(\text{CH}_3)_2$), 1.30 (d, $^3J_{\text{HH}} = 6.8$ Hz, 12 H, *p*- $\text{CH}(\text{CH}_3)_2$), 1.15 (d, $^3J_{\text{HH}} = 6.8$ Hz, 12 H, *o*- $\text{CH}(\text{CH}_3)_2$), 1.05 (d, $^3J_{\text{HH}} = 6.8$ Hz, 12 H, *o*- $\text{CH}(\text{CH}_3)_2$), –0.24 (s, $^2J_{\text{YH}} = 2.3$ Hz, 24 H, $\text{Al}(\text{CH}_3)_4$) ppm. ^{13}C NMR (151 MHz, C_6D_6 , 25 °C): $\delta = 149.0$ (*p*-Trip), 147.1 (*o*-Trip), 146.9 (ar), 135.4 (*i*-Trip), 133.4 (ar), 131.7 (ar), 128.5 (ar), 122.8 (ar), 121.9 (*m*-Trip), 120.9 (ar), 34.7 (*p*- $\text{CH}(\text{CH}_3)_2$), 30.8 (*o*- $\text{CH}(\text{CH}_3)_2$), 26.3 (*o*- $\text{CH}(\text{CH}_3)_2$), 24.5 (*p*- $\text{CH}(\text{CH}_3)_2$), 23.1 (*o*- $\text{CH}(\text{CH}_3)_2$), 3.5 (s br, $^1J_{\text{YC}} = 4.6$ Hz, $\text{Al}(\text{CH}_3)_4$) ppm. Anal. Calcd. for $\text{C}_{50}\text{H}_{78}\text{N}_3\text{Al}_2\text{Y}$: C, 69.50; H, 9.10; N, 4.86. Found: C, 69.21; H, 9.38; N, 4.80.

$[(\text{Tph})_2\text{N}_3]\text{La}(\text{AlMe}_4)_2$ (**2b**)

Following the protonolysis procedure described above, $\text{La}(\text{AlMe}_4)_3$ (**1b**, 80 mg, 0.20 mmol) and $[(\text{Tph})_2\text{N}_3]\text{H}$ (120 mg, 0.20 mmol) yielded **2b**, contaminated by **3**, as a powdery yellow

solid (193 mg, 49%, based on ^1H NMR). Salt metathesis gave a reaction yield of 51%. A small amount of pure product **2b** could be obtained by washing the mixture with cold hexane. ^1H NMR (400 MHz, C_6D_6 , 25 $^\circ\text{C}$): δ = 7.21 (s, 4 H, *m*-Trip), 7.14-7.19 (m, 2 H, ar), 7.05 (d, $^3J_{\text{HH}}$ = 7.6 Hz, 2 H, ar), 6.92 (t, $^3J_{\text{HH}}$ = 7.6 Hz, 2 H, ar), 6.81 (d, $^3J_{\text{HH}}$ = 8.0 Hz, 2 H, ar), 2.91 (sep, $^3J_{\text{HH}}$ = 6.8 Hz, 2 H, *p*- $\text{CH}(\text{CH}_3)_2$), 2.78 (sep, $^3J_{\text{HH}}$ = 6.8 Hz, 4 H, *o*- $\text{CH}(\text{CH}_3)_2$), 1.32 (d, $^3J_{\text{HH}}$ = 6.8 Hz, 12 H, *p*- $\text{CH}(\text{CH}_3)_2$), 1.15 (d, $^3J_{\text{HH}}$ = 6.8 Hz, 12 H, *o*- $\text{CH}(\text{CH}_3)_2$), 1.06 (d, $^3J_{\text{HH}}$ = 6.8 Hz, 12 H, *o*- $\text{CH}(\text{CH}_3)_2$), -0.15 (s, 24 H, $\text{Al}(\text{CH}_3)_4$) ppm. ^{13}C NMR (151 MHz, C_6D_6 , 25 $^\circ\text{C}$): δ = 34.6 (*p*- $\text{CH}(\text{CH}_3)_2$), 31.1 (*o*- $\text{CH}(\text{CH}_3)_2$), 25.6 (*o*- $\text{CH}(\text{CH}_3)_2$), 24.3 (*p*- $\text{CH}(\text{CH}_3)_2$), 23.5 (*o*- $\text{CH}(\text{CH}_3)_2$), 5.0 (s br, $\text{Al}(\text{CH}_3)_4$) ppm (the intensities of signals in the aromatic region were too low to be interpreted). Anal. Calcd. for $\text{C}_{50}\text{H}_{78}\text{N}_3\text{Al}_2\text{La}$: C, 65.70; H, 8.60; N, 4.60. Found: C, 65.16; H, 8.58; N, 4.48.

[(Tph) $_2\text{N}_3$]Nd(AlMe $_4$) $_2$ (**2c**)

Following the protonolysis procedure described above, Nd(AlMe $_4$) $_3$ (**1c**, 81 mg, 0.20 mmol) and [(Tph) $_2\text{N}_3$]H (120 mg, 0.20 mmol) yielded **2c**, contaminated by **3**, as a powdery greenish solid. Crystallization from hexane at -30 $^\circ\text{C}$ afforded light green single crystals of **2c** suitable for X-ray diffraction analysis (72 mg, 0.08 mmol, 39% from crystallization). IR (Nujol): 1610 w, 1569 w, 1460 vs (nujol), 1383 vs (Nujol), 1290 m, 1207 w, 1166 w, 1098 w, 1005 w, 943 w, 881 w, 757 m, 721 m, 664 w, 586 w cm^{-1} . Anal. Calcd. for $\text{C}_{50}\text{H}_{78}\text{N}_3\text{Al}_2\text{Nd}$: C, 65.32; H, 8.55; N, 4.57. Found: C, 65.37; H, 8.18; N, 4.38.

[(Tph) $_2\text{N}_3$]Lu(AlMe $_4$) $_2$ (**2d**)

Following the protonolysis procedure described above, Lu(AlMe $_4$) $_3$ (**1d**, 69 mg, 0.16 mmol) and [(Tph) $_2\text{N}_3$]H (95 mg, 0.16 mmol) yielded **2d**, contaminated by **3**, as a powdery yellow solid. Crystallization from hexane at -30 $^\circ\text{C}$ afforded yellow single crystals of **2d** suitable for X-ray diffraction analysis (55 mg,

0.06 mmol, 36% from crystallization). Salt metathesis gave a reaction yield of 37%. IR (Nujol): 1610 w, 1564 w, 1460 vs (Nujol), 1383 vs (Nujol), 1326 w, 1274 s, 1233 m, 1207 m, 1186 w, 1098 w, 1078 w, 1052 w, 1005 w, 938 w, 876 w, 757 m, 721 m, 710 m, 659 w, 591 w, 529 w cm^{-1} . ^1H NMR (600 MHz, C_6D_6 , 25 $^\circ\text{C}$): δ = 7.12-7.16 (m, 6 H, ar), 7.10 (d, $^3J_{\text{HH}}$ = 7.5 Hz, 2 H, ar), 6.93 (t, $^3J_{\text{HH}}$ = 7.5 Hz, 2 H, ar), 6.71 (d, $^3J_{\text{HH}}$ = 8.0 Hz, 2 H, ar), 2.87 (sep, $^3J_{\text{HH}}$ = 6.8 Hz, 2 H, *p*- $\text{CH}(\text{CH}_3)_2$), 2.84 (sep, $^3J_{\text{HH}}$ = 6.8 Hz, 2H, *o*- $\text{CH}(\text{CH}_3)_2$), 2.71 (sep, $^3J_{\text{HH}}$ = 6.8 Hz, 2 H, *o*- $\text{CH}(\text{CH}_3)_2$), 1.31 (d, $^3J_{\text{HH}}$ = 6.8 Hz, $\text{CH}(\text{CH}_3)_2$), 1.27 (d, $^3J_{\text{HH}}$ = 6.8 Hz, $\text{CH}(\text{CH}_3)_2$), 1.15 (d, $^3J_{\text{HH}}$ = 6.8 Hz, $\text{CH}(\text{CH}_3)_2$), 1.12 (d, $^3J_{\text{HH}}$ = 6.8 Hz, $\text{CH}(\text{CH}_3)_2$), 1.05 (d, $^3J_{\text{HH}}$ = 6.8 Hz, $\text{CH}(\text{CH}_3)_2$), -0.02 (s, 24 H, $\text{Al}(\text{CH}_3)_4$) ppm. Anal. Calcd. for $\text{C}_{50}\text{H}_{78}\text{N}_3\text{Al}_2\text{Lu}$: C, 63.21; H, 8.28; N, 4.42. Found: C, 63.81; H, 6.96; N, 4.22.

Synthesis of [(Tph) $_2\text{N}_3$]AlMe $_2$ (**3**)

In a glovebox, [(Tph) $_2\text{N}_3$]H (201 mg, 0.33 mmol) was suspended in 3 mL hexane and an excess AlMe $_3$ (49 μL , 0.51 mmol) was added *via* micropipette while stirring. Instant gas formation was observed, and the mixture turned from a light yellow suspension into a bright yellow, clear solution. The reaction mixture was stirred another 0.5 h at ambient temperature, and then dried under vacuum to yield a yellow powdery solid of **3** in quantitative yield (212 mg, 0.32 mmol, 98%). Crystallization from hexane at -30 $^\circ\text{C}$ afforded yellow single crystals of **3** suitable for X-ray diffraction analysis. IR (Nujol, cm^{-1}): 1610 w, 1569 w, 1460 vs (Nujol), 1378 vs (Nujol), 1290 vs, 1207 m, 1197 m, 1166 w, 1159 w, 1103 w, 1067 w, 1052 w, 1005 m, 938 w, 881 m, 762 s, 721 s, 710 s, 659 m, 591 w, 529 w cm^{-1} . ^1H NMR (400 MHz, C_6D_6 , 25 $^\circ\text{C}$): δ = 7.41 (d, $^3J_{\text{HH}}$ = 8.0 Hz, 2 H, ar), 7.17 (s, 4 H, *m*-Trip), 7.14-7.20 (m, 2 H, ar), 7.12 (d, $^3J_{\text{HH}}$ = 7.3 Hz, 2 H, ar), 6.98 (t, $^3J_{\text{HH}}$ = 7.3 Hz, 2 H, ar), 2.85 (sep, $^3J_{\text{HH}}$ = 6.8 Hz, 2 H, *p*- $\text{CH}(\text{CH}_3)_2$), 2.71 (sep, $^3J_{\text{HH}}$ = 6.8 Hz, 4 H, *o*- $\text{CH}(\text{CH}_3)_2$), 1.29 (d, $^3J_{\text{HH}}$ = 6.8 Hz, 12 H, *p*- $\text{CH}(\text{CH}_3)_2$), 1.18 (d, $^3J_{\text{HH}}$ = 6.8 Hz, 12 H, *o*- $\text{CH}(\text{CH}_3)_2$), 1.06 (d, $^3J_{\text{HH}}$ = 6.8 Hz, 12 H, *o*- $\text{CH}(\text{CH}_3)_2$), -0.99 (s, 6 H, $\text{Al}(\text{CH}_3)_2$) ppm. ^{13}C NMR (151 MHz, C_6D_6 , 25 $^\circ\text{C}$): δ = 149.2 (*p*-Trip), 147.0 (*o*-Trip), 143.9

Table 6 Crystal Data and Data Collection Parameters of Complexes **2a**, **2c**, **2d** and **3**

	2a	2c	2d	3
Chemical formula	$\text{C}_{106}\text{H}_{170}\text{N}_6\text{Al}_4\text{Y}_2$	$\text{C}_{50}\text{H}_{78}\text{N}_3\text{Al}_2\text{Nd}$	$\text{C}_{106}\text{H}_{170}\text{N}_6\text{Al}_4\text{Lu}_2$	$\text{C}_{44}\text{H}_{60}\text{N}_3\text{Al}$
Formula Mass	1814.22	919.35	1986.34	657.93
Crystal system	Monoclinic	Monoclinic	Monoclinic	Monoclinic
<i>a</i> / \AA	10.0997(2)	22.4306(13)	10.0659(3)	16.9941(7)
<i>b</i> / \AA	51.7483(12)	9.5164(5)	51.7349(14)	13.1084(5)
<i>c</i> / \AA	20.7090(5)	25.0736(14)	20.7342(6)	17.6874(7)
<i>alpha</i> / $^\circ$	90.00	90.00	90.00	90.00
<i>beta</i> / $^\circ$	94.419(1)	107.802(1)	94.371(1)	97.496(1)
<i>gamma</i> / $^\circ$	90.00	90.00	90.00	90.00
Unit cell volume/ \AA^3	10791.2(4)	5095.9(5)	10766.1(5)	3906.5(3)
<i>T</i> /K	100(2)	100(2)	123(2)	100(2)
Space group	$P2_1/n$	$P2_1/c$	$P2_1/n$	$P2_1/n$
No. of formula units per unit cell, <i>Z</i>	4	4	4	4
No. of independent reflections	19067	9684	18995	8687
Final R_1 values ^a	0.0614	0.0553	0.0669	0.0473
Final $wR_2(F^2)$ values ^a	0.1178	0.1313	0.1073	0.0995
Final R_1 values (all data) ^a	0.0866	0.0677	0.0980	0.0639
Final $wR_2(F^2)$ values (all data) ^a	0.1263	0.1376	0.1150	0.1066
Goodness of fit on F^2 ^a	1.137	1.065	1.156	1.041

^a $R_1 = \sum(\|F_o\| - |F_c|)/\sum|F_o|$; $wR_2 = \{\sum[w(F_o^2 - F_c^2)^2]/\sum[w(F_o^2)^2]\}^{1/2}$; GOF = $\{\sum[w(F_o^2 - F_c^2)^2]/(n-p)\}$

(ar), 134.4 (*i*-Trip), 132.6 (ar), 132.1 (ar), 128.6 (ar), 125.4 (ar), 121.6 (*m*-Trip), 120.0 (ar), 35.0 (*p*-CH(CH₃)₂), 31.0 (*o*-CH(CH₃)₂), 25.6 (*o*-CH(CH₃)₂), 24.4 (*p*-CH(CH₃)₂), 23.3 (*o*-CH(CH₃)₂), -11.1 (Al(CH₃)₂) ppm. Anal. Calcd. for C₄₄H₆₀N₃Al: C, 80.32; H, 9.19; N, 6.39. Found: C, 80.25; H, 10.20; N, 6.10.

General procedure for the polymerization of isoprene

A detailed polymerization procedure (Table 4, run 18) is described as a typical example. [Ph₃C][B(C₆F₅)₄] (18 mg, 0.02 mmol, 1 equiv) was added to a solution of **2b** (18 mg, 0.02 mmol) in toluene (8 mL) and the mixture was aged at ambient temperature for 30 min. After the addition of isoprene (2.0 mL, 20 mmol), the polymerization was carried out at ambient temperature for 24 h. The reaction was terminated by pouring the polymerization mixture into a large quantity of acidified 2-propanol containing 0.1% (w/w) 2,6-di-*tert*-butyl-4-methylphenol as a stabilizer. The polymer was washed with 2-propanol and dried under vacuum at ambient temperature to constant weight. The polymer yield was determined gravimetrically.

X-ray crystallography and crystal structure determination of **2a**, **2c**, **2d**, and **3**

Crystals suitable for diffraction experiments were selected in a glovebox and mounted in Paratone-N (Hampton Research) inside a nylon loop. Data collection was done on a Bruker AXS SMART 2 K CCD diffractometer using graphite-monochromated Mo-K α radiation ($\lambda = 0.71073$ Å) performing ω -scans in four φ positions. Raw data were collected using the SMART software package,³⁸ and reduced and scaled with the SAINT program.³⁹ Numerical absorption corrections were done using SHELXTL.⁴⁰ The structures were solved by direct methods and refined with standard difference Fourier techniques.⁴⁰ All plots were generated using the ORTEP-3 program.⁴¹ For further experimental details on refinement and crystallographic data see Table 6.

Acknowledgements

Financial support from the Norwegian Research Council (Project No. 182547/I30) and the Deutsche Forschungsgemeinschaft (SPP 1166) is gratefully acknowledged.

Notes and references

- (a) F. T. Edelmann, *Chem. Soc. Rev.*, 2009, **38**, 2253; (b) F. T. Edelmann, D. M. M. Freckmann and H. Schumann, *Chem. Rev.*, 2002, **102**, 1851; (c) W. E. Piers and D. J. H. Emslie, *Coord. Chem. Rev.*, 2002, **233–234**, 131; (d) L. H. Gade, *Acc. Chem. Res.*, 2002, **35**, 575; (e) R. Kempe, *Angew. Chem., Int. Ed.*, 2000, **39**, 468.
- (a) P. M. Zeimentz, S. Arndt, B. R. Elvidge and J. Okuda, *Chem. Rev.*, 2006, **106**, 2404; (b) S. J. Park, Y. Y. Han, S. K. Kim, J. S. Lee, H. K. Kim and Y. K. Do, *J. Organomet. Chem.*, 2004, **689**, 4263; (c) V. C. Gibson and S. K. Spitzmesser, *Chem. Rev.*, 2003, **103**, 283.
- (a) L. Zhang, M. Nishiura, M. Yuki, Y. Luo and Z. Hou, *Angew. Chem., Int. Ed.*, 2008, **47**, 2642; (b) S. Bambirra, M. W. Bouwkamp, A. Meetsma and B. Hessen, *J. Am. Chem. Soc.*, 2004, **126**, 9182; (c) S. Bambirra, D. van Leusen, A. Meetsma, B. Hessen and J. H. Teuben, *Chem. Commun.*, 2003, 522.
- P. G. Hayes, W. E. Piers and R. McDonald, *J. Am. Chem. Soc.*, 2002, **124**, 2132.
- (a) C. Döring, W. P. Kretschmer, T. Bauer and R. Kempe, *Eur. J. Inorg. Chem.*, 2009, 4255; (b) M. Zimmermann, K. W. Törnroos, R. M. Waymouth and R. Anwander, *Organometallics*, 2008, **27**, 4310; (c) W. P. Kretschmer, A. Meetsma, B. Hessen, T. Schmalz, S. Qayyum and R. Kempe, *Chem.–Eur. J.*, 2006, **12**, 8969.
- (a) S. Bambirra, D. van Leusen, C. G. J. Tazelaar, A. Meetsma and B. Hessen, *Organometallics*, 2007, **26**, 1014; (b) S. Bambirra, D. van Leusen, A. Meetsma, B. Hessen and J. H. Teuben, *Chem. Commun.*, 2001, 637.
- (a) S. Li, D. Cui, D. Li and Z. Hou, *Organometallics*, 2009, **28**, 4814; (b) D. Wang, S. H. Li, X. L. Liu, W. Gao and D. Cui, *Organometallics*, 2008, **27**, 6531; (c) S. Li, W. Miao, T. Tang, W. Dong, X. Zhang and D. Cui, *Organometallics*, 2008, **27**, 718; (d) Y. Yang, Q. Wang and D. Cui, *J. Polym. Sci., Part A: Polym. Chem.*, 2008, **46**, 5251; (e) Y. Yang, B. Liu, K. Lv, W. Gao, D. Cui, X. Chen and X. Jing, *Organometallics*, 2007, **26**, 4575; (f) Y. Luo, M. Nishiura and Z. Hou, *J. Organomet. Chem.*, 2007, **692**, 536.
- (a) A. G. M. Barrett, M. R. Crimmin, M. S. Hill, P. B. Hitchcock, G. Kociok-Köhn and P. A. Procopiou, *Inorg. Chem.*, 2008, **47**, 7366; (b) S. Brase, S. Dahmen, F. Lauterwasser, N. E. Leadbeater and E. L. Sharp, *Bioorg. Med. Chem. Lett.*, 2002, **12**, 1849.
- S.-O. Hauber, F. Lissner, G. B. Deacon and M. Niemeyer, *Angew. Chem., Int. Ed.*, 2005, **44**, 5871.
- D. Pfeiffer, I. A. Guzei, L. M. Liabe-Sands, M. J. Heeg, A. L. Rheingold and C. H. Winter, *J. Organomet. Chem.*, 1999, **588**, 167.
- S. O. Hauber and M. Niemeyer, *Inorg. Chem.*, 2005, **44**, 8644.
- B. Liu and D. Cui, *Dalton Trans.*, 2009, 550.
- W. J. Evans, T. J. Mueller and J. W. Ziller, *J. Am. Chem. Soc.*, 2009, **131**, 2678.
- (a) M. Zimmermann, J. Takats, G. Kiel, K. W. Törnroos and R. Anwander, *Chem. Commun.*, 2008, 612; (b) R. Litlabø, M. Zimmermann, K. Saliu, J. Takats, K. W. Törnroos and R. Anwander, *Angew. Chem., Int. Ed.*, 2008, **47**, 9560; (c) M. Zimmermann, K. W. Törnroos and R. Anwander, *Angew. Chem., Int. Ed.*, 2007, **46**, 3126; (d) M. Zimmermann, F. Estler, E. Herdtweck, K. W. Törnroos and R. Anwander, *Organometallics*, 2007, **26**, 6029; (e) M. Zimmermann, K. W. Törnroos and R. Anwander, *Organometallics*, 2006, **25**, 3593.
- M. Zimmermann, K. W. Törnroos, H. Sitzmann and R. Anwander, *Chem.–Eur. J.*, 2008, **14**, 7266.
- H. S. Lee and M. Niemeyer, *Inorg. Chem.*, 2006, **45**, 6126.
- E. Le Roux, F. Nief, F. Jaroschik, K. W. Törnroos and R. Anwander, *Dalton Trans.*, 2007, 4866.
- (a) D. Vinduš and M. Niemeyer, unpublished results, and ref. 16 (Supporting Information); (b) H. S. Lee, S.-O. Hauber, D. Vinduš and M. Niemeyer, *Inorg. Chem.*, 2008, **47**, 4401; (c) H. S. Lee and M. Niemeyer, *Inorg. Chem.*, 2010, **49**, 730.
- R. Duchateau, C. T. vanWee, A. Meetsma, P. T. vanDuijnen and J. H. Teuben, *Organometallics*, 1996, **15**, 2279.
- C. Döring and R. Kempe, *Eur. J. Inorg. Chem.*, 2009, 412.
- W. J. Evans, R. Anwander and J. W. Ziller, *Organometallics*, 1995, **14**, 1107.
- M. Zimmermann, N. Å. Frøystein, A. Fischbach, P. Sirsch, H. M. Dietrich, K. W. Törnroos, E. Herdtweck and R. Anwander, *Chem.–Eur. J.*, 2007, **13**, 8784.
- H. M. Dietrich, E. Herdtweck, R. Anwander, unpublished results.
- H. M. Dietrich, O. Schuster, K. W. Törnroos and R. Anwander, *Angew. Chem., Int. Ed.*, 2006, **45**, 4858.
- R. Lechler, H. D. Hausen and J. Weidlein, *J. Organomet. Chem.*, 1989, **359**, 1.
- M. P. Coles, D. C. Swenson, R. F. Jordan and V. G. Young, *Organometallics*, 1997, **16**, 5183.
- B. X. Qian, D. L. Ward and M. R. Smith, *Organometallics*, 1998, **17**, 3070.
- C. E. Radzewich, M. P. Coles and R. F. Jordan, *J. Am. Chem. Soc.*, 1998, **120**, 9384.
- D. Vidovic, J. N. Jones, J. A. Moore and A. H. Cowley, *Z. Anorg. Allg. Chem.*, 2005, **631**, 2888.
- H. M. Dietrich, C. Zapilko, E. Herdtweck and R. Anwander, *Organometallics*, 2005, **24**, 5767.
- H. M. Dietrich, G. Raudaschl-Sieber and R. Anwander, *Angew. Chem., Int. Ed.*, 2005, **44**, 5303.
- The reaction mixture [(Tph)₂N₃]AlMe₂ + [Ph₃C][B(C₆F₅)₄] did in fact yield a precipitate in the attempted isoprene polymerization, which could be isolated as a white powder. However, by NMR and SEC investigations we could exclude the possibility of this being any form of polyisoprene. Attempts to characterize this compound have not yet been successful.

-
- 33 S. Arndt, K. Beckerle, P. M. Zeimentz, T. P. Spaniol and J. Okuda, *Angew. Chem., Int. Ed.*, 2005, **44**, 7473.
- 34 C. Meermann, K. W. Törnroos, W. Nerdal and R. Anwender, *Angew. Chem., Int. Ed.*, 2007, **46**, 6508.
- 35 A. Fischbach, M. G. Klimpel, M. Widenmeyer, E. Herdtweck, W. Scherer and R. Anwender, *Angew. Chem., Int. Ed.*, 2004, **43**, 2234.
- 36 All systems show bimodal distributions with closely overlapping peaks.
- 37 L. Zhang, T. Suzuki, Y. Luo, M. Nishiura and Z. Hou, *Angew. Chem., Int. Ed.*, 2007, **46**, 1909.
- 38 SMART v. 5.054, *Data Collection Software for Bruker AXS CCD*, Bruker AXS Inc., Madison, WI, 1999.
- 39 SAINT v. 6.45a, *Data Integration Software for Bruker AXS CCD*, Bruker AXS Inc., Madison, WI, 2002.
- 40 SHELXTL v. 6.14, *Structure Determination Software Suite*, Bruker AXS Inc., Madison, WI, 2000.
- 41 L. J. Farrugia, *J. Appl. Crystallogr.*, 1997, **30**, 565.